Analysis of Fission with Selective Channel Scission Model

Masayuki OHTA and Shoji NAKAMURA
Japan Atomic Energy Agency
2-4 Shirakata-Shirane, Tokai-mura, Naka-gun, Ibaraki, 319-1195, Japan
E-mail: ohta.masayuki@jaea.go.jp

The mass distributions of fission product yields for neutron-induced fissions of ^{232}Th, ^{235}U, ^{239}Pu and ^{241}Pu were calculated by the selective channel scission model with simple assumptions. Although the present calculation is a rough estimation, it is applicable to the wide range of fissionable nuclei without the adjustable parameters for each fission channel.

1. Introduction

The multimodal random-neck rupture model [1], which based on the assumption of the existence of few fission paths (modes), has been used for fission analyses as the standard. Recently, the five-dimensional analysis [2] revealed the existence of symmetric and asymmetric paths of fission. There are some improvements and developments for fission analysis. However, there still remain difficulties in prediction of the fission product (FP) yields about which there are no experimental data. Therefore, the selective channel scission (SCS) model [3-5] has been proposed to calculate the fission product yield. This model deals with the fission process for each channel. The fission product yields are calculated from the penetrabilities of the channel-dependent fission barriers. Since the channel-dependent fission barrier has not been calculated theoretically yet, the adjustable parameters which are concerned with the elongation and the deformation of the nucleus and the Coulomb potential between two fission fragments have been introduced to calculate the channel-dependent fission barrier.

This paper gives the results for fission product yields obtained by SCS model with the simple assumptions, and discusses the correlation between the parameter and the fission modes on the multimodal random-neck rupture model.

2. Model Assumptions and Calculations

The fission process and the potential are shown in **Fig. 1**. The excited nucleus is deformed, and induces tandem (dumbbell) oscillation collectively. It starts scission to form two fission fragments (FP1 and FP2). Here, the following fission potentials are considered for all fission channels. The channel-dependent fission barrier E_f is estimated from the difference between the Q-value and the potential at the saddle point

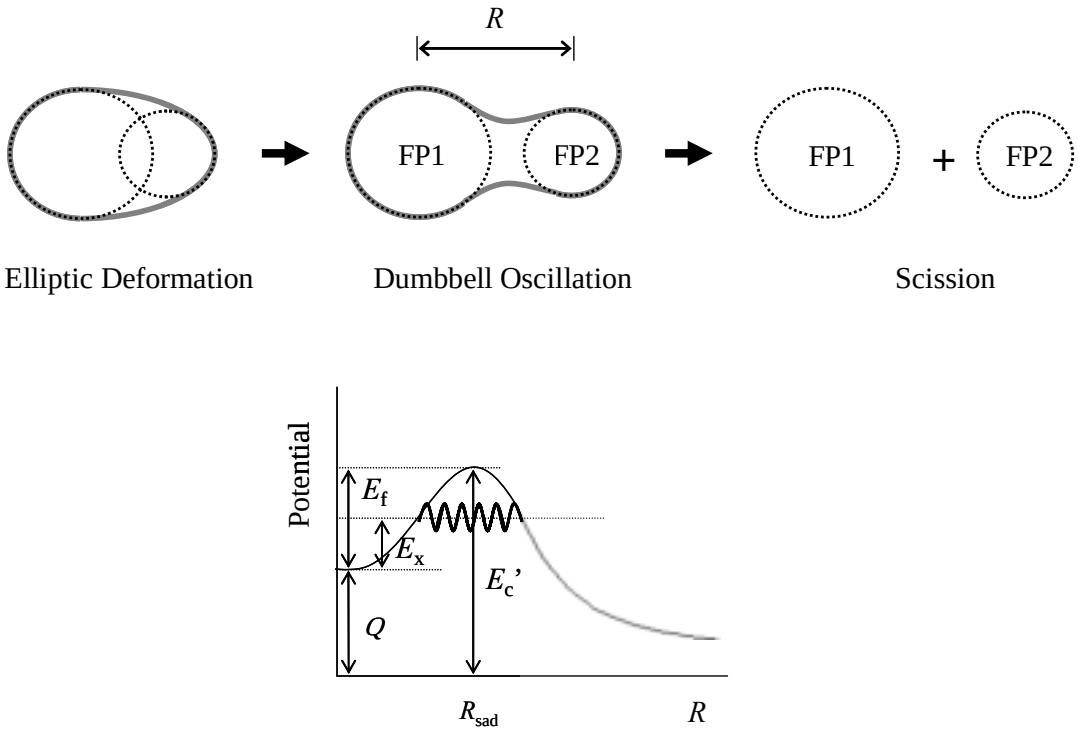

Fig. 1 Fission process and potential.

R_{sad}. In this work, the E_f is calculated with simple assumptions described below.

The potential at R_{sad} is estimated from the Coulomb potential between two fission fragments of the certain channel. It assumes that the R_{sad} is given by the sum of the radii of two fragments at the grand state ($R_1^{'}$ and $R_2^{'}$) and the distance of the nuclear interaction ($\Delta \approx 2$ fm).

$$R_{sad} = R_1^{'} + R_2^{'} + \Delta. \tag{1}$$

For the deformations of nuclei, the data of KTUY mass formula [6] were used in this analysis. The value of R_{sad} approximately corresponds to the interaction distance of the nuclear reaction. The Coulomb barrier is given by Eq. (2),

$$E_c^{'} = \frac{1.44\,Z_1 Z_2}{R_{sad}}, \tag{2}$$

in MeV and fm units, where Z_1 and Z_2 are the atomic number of the fragments FP1 and FP2, respectively.

The channel-dependent barrier E_f is defined as follows,

$$E_f = E_c^{'} - Q. \tag{3}$$

It assumes that the potential height at the saddle point is nearly equal to the Coulomb barrier of fusion as the reversal process of fission.

The fission probability for the certain channel is given by the tunnel probability P of the channel-dependent potential for the excitation energy E_x,

$$P = \frac{1}{1+\exp\left[\frac{2}{\hbar}\int_a^b \sqrt{2M(s)(V(s)-E_x)}\,ds\right]}, \tag{4}$$

where s is the distance along the fission path, $V(s)$ is the potential energy, a and b are the points at which $V(s) = E_x$ and $M(s)$ is the mass parameter of the system. The potential near the saddle point is approximated by the inverted parabola and the curvatures α is assumed as a constant for all channels for simplicity. Then the tunnel probability P is reduced as

$$P \approx \frac{1}{1+\exp\left[0.218\alpha\sqrt{\mu}\ \Delta E\right]}, \tag{5}$$

in MeV and fm units, where $\mu = \mathrm{A}_1\mathrm{A}_2/(\mathrm{A}_1+\mathrm{A}_2)$, $\Delta E = E_f - E_x$ and A_1 and A_2 are the mass number of FP1 and FP2, respectively. The FP yields are obtained by summing up these probabilities all over fission channels.

Furthermore, the η is introduced to discuss how much the nucleus deviates from the spherical shape. The η is defined as the elongation at the saddle point from the point-to-point distance of the fission fragment of spherical shapes which is given by

$$R_{\mathrm{sad}} = \eta(R_1 + R_2), \tag{6}$$

where R_1 and R_2 are the radii of FP1 and FP2, respectively, and given as $R_1 = r_0\mathrm{A}_1^{1/3}$, $R_2 = r_0\mathrm{A}_2^{1/3}$ and $r_0 = 1.2$ fm.

3. Results and Discussion

The FP yields for the neutron-induced fissions of ^{232}Th, ^{235}U, ^{239}Pu and ^{241}Pu were obtained as shown in **Figs. 2-a**, **3-a**, **4-a** and **5-a**, respectively. Prompt neutron emission was considered only for the FP yields for ^{235}U. Others show the FP yields without the consideration of the prompt neutron emission. The position of the humps coincided with the data of JENDL-3.3 [7] except for the dips in the mass region of A = 140–150 (also A = 85–95). The channel-dependent fission barriers E_f for ^{233}Th, ^{236}U, ^{240}Pu and ^{242}Pu were shown in **Figs. 2-b**, **3-b**, **4-b** and **5-b**, respectively. The dips of E_f corresponding to the yields of mass region of A = 140–150 (also A = 85–95) were found.

Figures 2-c, **3-c**, **4-c** and **5-c** shows the η for ^{233}Th, ^{236}U, ^{240}Pu and ^{242}Pu, respectively. The dips of the FP yields and E_f in A = 140–150 (also A = 85–95) may depend on the differences between the real distance at saddle point and the assumption of R_{sad}. The upper part of the η increases around A = 130–140 with the mass number of fragments. The η is discussed in connection with the shape elongation at scission. Y.L. Zhao *et al*. [8] showed the existence of symmetric and asymmetric fissions with the factor β, which is the ratio of the elongation from sphere nuclei at scission configurations, by evaluation from the total kinetic energy (TKE) data. The β changed the trend at mass of fragments A ~ 130. The behavior of η also changes its trend around A = 130–140 like that of the β.

4. Conclusions

The channel-dependent fission barrier was calculated for the neutron-induced fissions of ^{232}Th, ^{235}U, ^{239}Pu and ^{241}Pu by the SCS model with simple assumptions. The mass distributions of FP yields were calculated and compared with the data of JENDL-3.3 [7]. These mass yields were in agreement with the data of JENDL-3.3 except for discrepancies at the mass regions of A = 140–150 (also A = 85–95). To improve the discrepancies, further studies should be needed for the model calculation and assumptions.

The elongation factor at saddle point η was calculated and compared with that at scission point β in Ref. [8]. Though the deviation was wide, the trend of η was similar to that of the β. It might mean the existence of the symmetric and asymmetric fission modes for the η as well as that for the β.

References

[1] U. Brosa, S. Grosmann and A. Müller: *Phys. Rep.*, **197**, 167 (1990).

[2] P. Möller, D.G. Madland, A.J. Sierk and A. Iwamoto: *Nature*, **409**, 785 (2001).

[3] A. Takahashi, M. Ohta and T. Mizuno: *Jpn. J. Appl. Phys.*, **40**, 7031 (2001).

[4] M. Ohta, M. Matsunaka and A. Takahashi: *Jpn. J. Appl. Phys.*, **40**, 7047 (2001).

[5] M. Ohta and A. Takahashi: *Jpn. J. Appl. Phys.*, **42**, 645 (2003).

[6] H. Koura, M. Uno, T. Tachibana and M. Yamada: *Nucl. Phys.*, **A674**, 47 (2000).

[7] K. Shibata, T. Kawano, T. Nakagawa, O. Iwamoto, J. Katakura, T. Fukahori, S. Chiba, A. Hasegawa, T. Murata, H. Matsunobu, T. Ohsawa, Y. Nakajima, T. Yoshida, A. Zukeran, M. Kawai, M. Baba, M. Ishikawa, T. Asami, T. Watanabe, Y. Watanabe, M. Igashira, N. Yamamuro, H. Kitazawa, N. Yamano and H. Takano: *J. Nucl. Sci. and Technol.*, **39**, 1125 (2002).

[8] Y.L. Zhao, I. Nishinaka, Y. Nagame, M. Tanikawa, K. Tsukada, S. Ichikawa, K. Sueki, Y. Oura, H. Ikezoe, S. Mitsuoka, H. Kudo, T. Ohtsuki and H. Nakahara: *Phys. Rev. Lett.*, **82**, 3408 (1999).

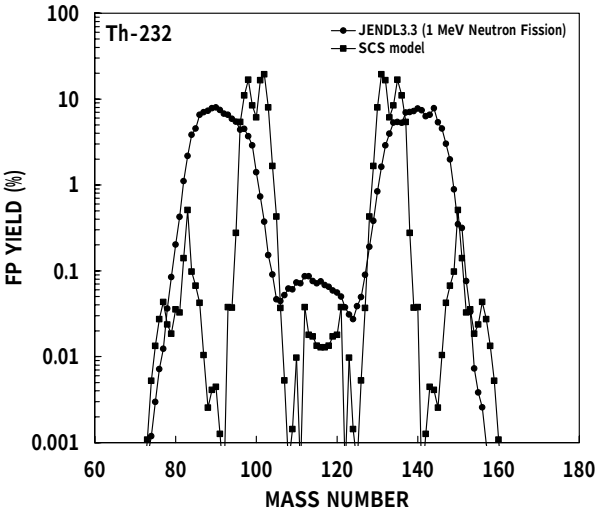

Fig. 2-a Fission product yield of n+^{232}Th

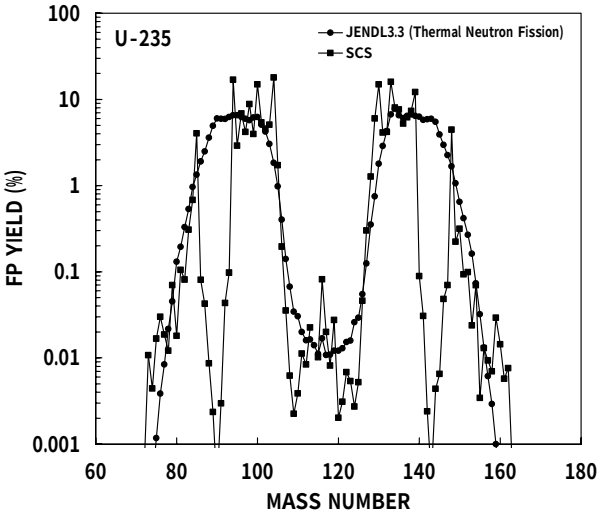

Fig. 3-a Fission product yield of n+^{235}U

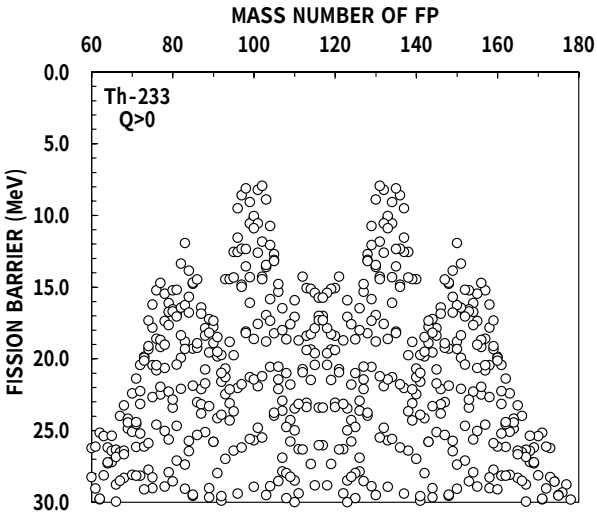

Fig. 2-b Fission barriers of ^{233}Th

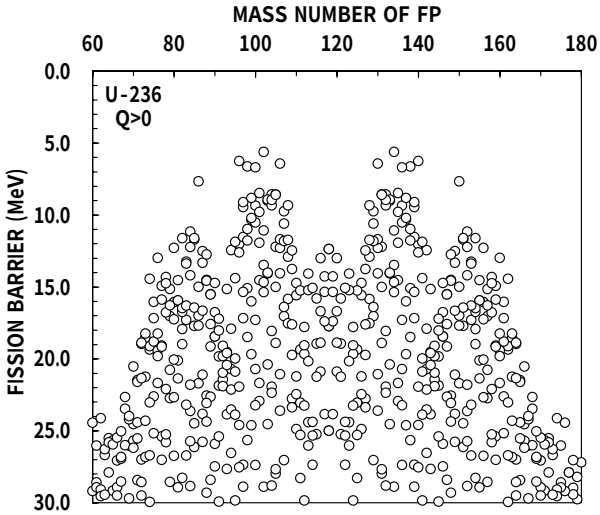

Fig. 3-b Fission barriers of ^{236}U

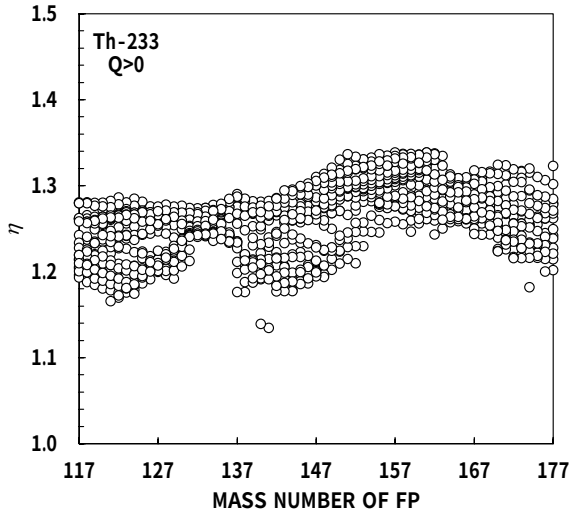

Fig. 2-c η of ^{233}Th

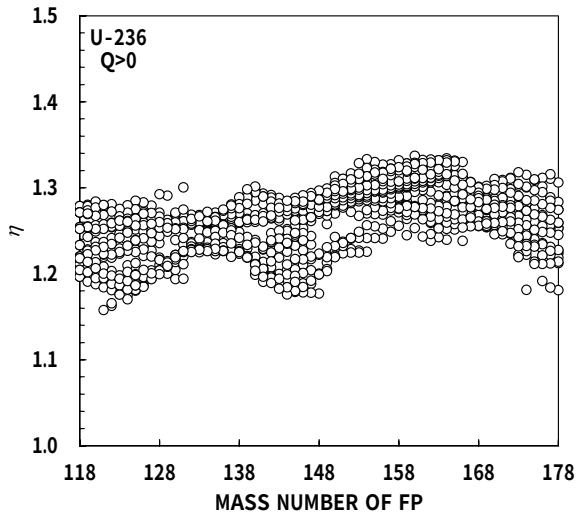

Fig. 3-c η of ^{236}U

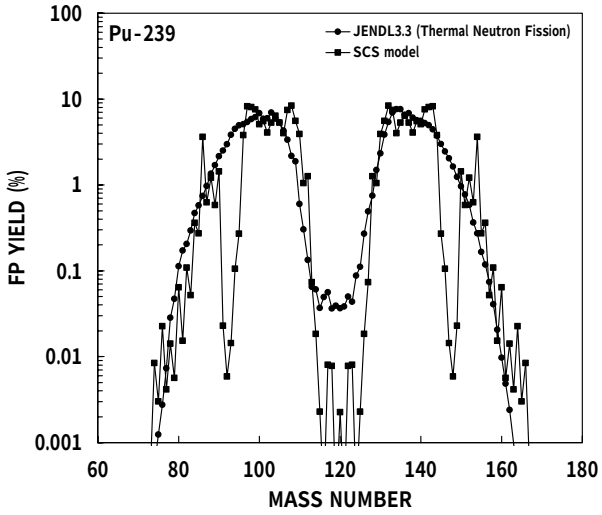

Fig. 4-a Fission product yield of n+^{239}Pu

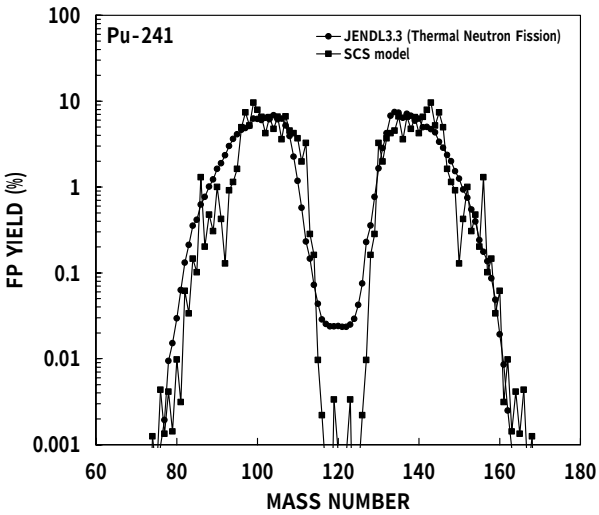

Fig. 5-a Fission product yield of n+^{241}Pu

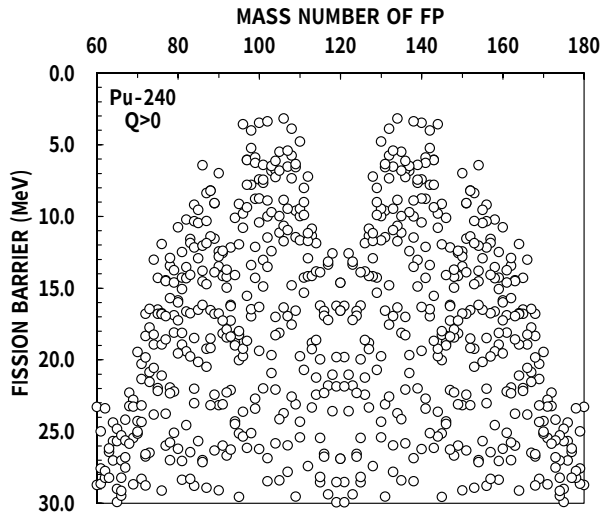

Fig. 4-b Fission barriers of ^{240}Pu

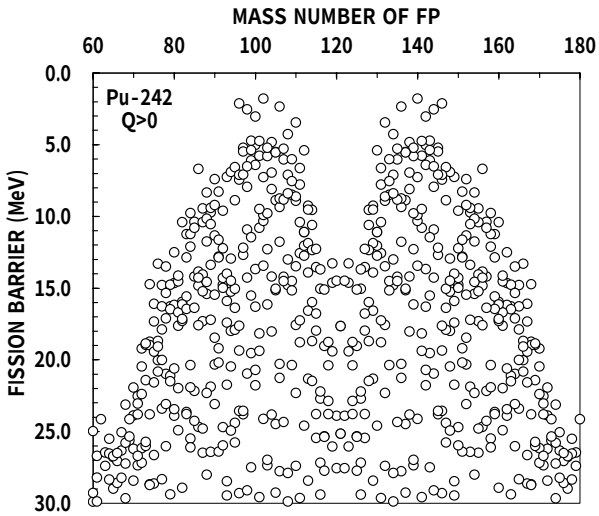

Fig. 5-b Fission barriers of ^{242}Pu

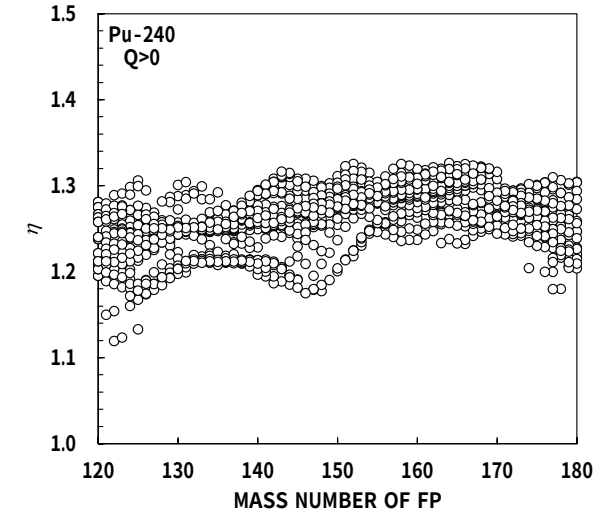

Fig. 4-c η of ^{240}Pu

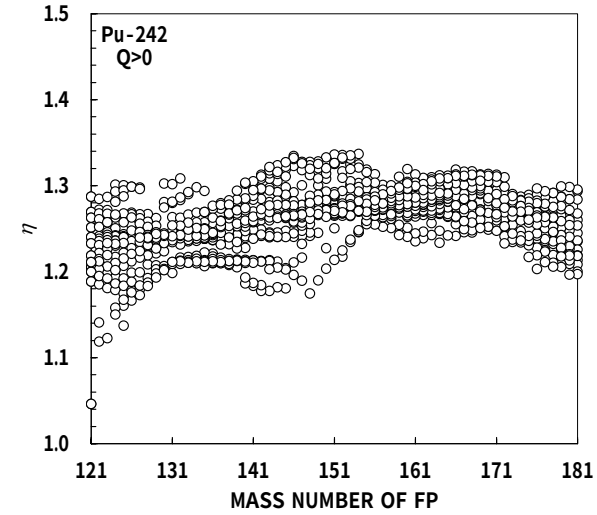

Fig. 5-c η of ^{242}Pu